Structural analysis and tissue localization of human C4.4A: a protein homologue of the urokinase receptor

Line V. HANSEN*, Henrik GÅRDSVOLL*, Boye S. NIELSEN*, Leif R. LUND*, Keld DANØ*, Ole N. JENSEN† and Michael PLOUG*[1]

*Finsen Laboratory, Rigshospitalet, Strandboulevarden 49, DK-2100 Copenhagen, Denmark, and †Department of Biochemistry and Molecular Biology, University of Southern Denmark, Campusvej 55, DK-5230 Odense M, Denmark

C4.4A, a structural homologue of the urokinase-type plasminogen activator receptor (uPAR), was originally identified as a metastasis-associated membrane protein, but little is known about its structural and functional properties. Therefore, we expressed, purified and characterized a soluble truncated form of human C4.4A, and used this protein to produce specific polyclonal anti-C4.4A antibodies. By immunohistochemistry we observed a pronounced surface staining for C4.4A in suprabasal keratinocytes of chronic human wounds and found C4.4A expression markedly upregulated in migrating keratinocytes during re-epithelisation of incisional skin wounds. Phorbol-ester-induced hyperplasia of mouse skin is also accompanied by a significant induction of C4.4A expression in the multilayered, suprabasal keratinocytes. C4.4A contains two Ly-6 (leucocyte antigen 6)/uPAR/α-neurotoxin modules. Our recombinant human C4.4A is extensively modified by post-translational glycosylation, which include 5–6 N-linked carbohydrates primarily located in or close to its second Ly-6/uPAR/α-neurotoxin module and approximately 15 O-linked carbohydrates clustered in a Ser/Thr/Pro-rich region at the C-terminus. A highly protease-sensitive region (Tyr^{200}–Arg^{204}) is located between these two clusters of N- and O-linked carbohydrates. The natural, glycolipid-anchored C4.4A from amnion membranes of human term placenta exhibits similar properties. Using recombinant, soluble C4.4A or MCF 7 cells, which express significant amounts of GPI-anchored C4.4A, we find no evidence for an interaction between C4.4A and uPA, a property suggested previously for rat C4.4A. Collectively these data indicate that C4.4A, although being a structural homologue of uPAR, is unlikely to have a functional overlap with uPAR.

Key words: GPI-anchor, O-linked glycosylation, suprabasal keratinocytes, uPA, uPAR domain family, wound healing.

INTRODUCTION

Identification of genes that are upregulated during malignant tumour progression and metastasis is of fundamental importance for the dissection of the operational molecular mechanisms during the progression of cancer. Obviously, detailed biochemical studies are needed on such gene products to select those which may serve as targets for the development of a protein-specific intervention strategy beneficial to cancer patient management. Using two unrelated differential display methods, designed to select genes that are up-regulated in cancer, two independent research laboratories recently identified C4.4A [1,2]. Exploiting the differential antigenicity between a metastasizing and a non-metastasizing sub-clone of a rat pancreatic tumour-cell line, Zöller and co-workers [1] were the first to classify C4.4A as a cancer-associated membrane protein. The orthologous human gene encoding C4.4A was subsequently identified and assigned to chromosome 19 [3]. Independently, Southgate and co-workers [2] also demonstrated that the gene for C4.4A was differentially upregulated in human urothelial cells when these were grown on extracellular matrix proteins, compared with plastic. This *in vitro* model system is believed to partially mimic the normal inducible wound response in the healing urothelium and may also have some bearing on transitional cell carcinoma [2]. A correlation between C4.4A expression and malignant progression of human melanomas has been reported recently [4].

Analyses of the cDNA-derived sequences for rat and human C4.4A, with special emphasis on the spacing of cysteine residues, clearly assign C4.4A to the Ly-6 (leucocyte antigen 6)/uPAR (urokinase-type plasminogen activator receptor)/α-neurotoxin protein domain family with a particular resemblance to the receptor for urokinase-type plasminogen activator [1,3,5,6]. Both proteins are attached to the cell membrane by a glycosyl-phosphatidylinositol (GPI) anchor [1,7] and both are multidomain proteins; however, C4.4A contains two Ly-6/uPAR/α-neurotoxin domains compared with the three present in uPAR [5,6]. Furthermore, the genes encoding human C4.4A and uPAR are both located on chromosome 19q13.2 [3,8], only 180 kb apart according to the human genome project (http://www.ncbi.nlm.nih.gov/mapview/maps.cgi?org=hum&chr=19).

Little is presently known about the functional properties of C4.4A. However, it has been proposed that it plays a role in either cell–cell or cell–matrix interactions because its gene expression is inducible by exposure to extracellular matrix proteins, but a causal relationship for this has not been established [2]. Consistently it was reported that a rat tumour cell line transiently binds to laminin and penetrates through a Matrigel® in processes depending on constitutive C4.4A expression [1]. Finally, it was also suggested that rat C4.4A, through binding of rat uPA (urokinase-type plasminogen activator), could be involved in proteolytic degradation of the extracellular matrix [1]. The latter proposal is especially interesting with a view to the fairly mild phenotypes

Abbreviations used: Caps, 3-(cyclohexylamino)propane-1-sulphonic acid; C4.4A′, truncated fragment of C4.4A; GPI, glycosyl-phosphatidylinositol; hAG, human anterior gradient; Ly-6, leucocyte antigen 6; MALDI–TOF-MS, matrix-assisted laser-desorption ionization–time-of-flight mass spectrometry; PI-PLC, phosphatidyl-inositol specific phospholipase C; pro-uPA, the zymogen of uPA; SFM, serum free medium; S2 cells, Schneider 2 cells from *Drosophila melanogaster*; STP-rich, serine, threonine and proline rich; suPAR, soluble uPA receptor; uPA, urokinase-type plasminogen activator; uPAR, uPA receptor; uPAR DIII, uPAR domain III.

[1] To whom correspondence should be addressed (e-mail m-ploug@finsenlab.dk).

presented so far by the gene targeted uPAR$^{-/-}$ mice [9,10]. The urokinase receptor has been implicated in cancer invasion and metastasis through its contributions to focalised plasminogen activation at the cell surface by its high affinity for uPA and to cell adhesion by its interplay with vitronectin and some integrins (for review see [6]).

In the present study therefore, we expressed, purified and characterized a soluble recombinant form of human C4.4A, and developed polyclonal antibodies specific for C4.4A, thus enabling us to investigate further structural and functional properties of C4.4A.

EXPERIMENTAL

Chemicals and reagents

cDNA encoding human C4.4A was a gift from Dr M. Zöller (Department of Tumour Progression and Immune Defence, Heidelberg, Germany) [3]. Soluble recombinant human uPAR were expressed in *Drosophila* S2 cells and purified from conditioned medium as described previously [11]. Recombinant human pro-uPA (the zymogen of uPA) expressed in *Escherichia coli* was kindly provided by Dr D. Saunders (Grünenthal, Germany). Vitronectin was obtained from Calbiochem (San Diego, CA, U.S.A.). Recombinant enterokinase (EC 3.4.21.9) was from Stratagene (La Jolla, CA, U.S.A.). Chymotrypsin (EC 3.4.21.1) was from Worthington Biochemical Corp. (Lakewood, NJ, U.S.A.). Modified trypsin (EC 3.4.21.4) was obtained from Promega (Madison, WI, U.S.A.). Recombinant *Flavobacterium meningosepticum* N-glycanase (EC 3.2.2.18) expressed in *E. coli*. (25 units/μg), O-glycosidase (EC 3.2.1.97) from *Diplococcus pneumoniae*, PI-PLC (phosphatidyl-inositol specific phospholipase C) from *Bacillus cereus* (600 units/mg), and the following digoxigenin-labelled lectins: Con A (from *Canavalia ensiformis*), AAA (from *Aleuria aurantia*) and PNA (from *Arachis hypogaea*) were all from Roche A/S (Basel, Switzerland).

WesternBreeze™, RPMI media, CellFectin, hygromycin, *Drosophila* serum free medium (SFM), and the vectors pMT/V5-His and pCoHygro were obtained from Invitrogen (Groningen, The Netherlands). T7 RNA polymerase and *Sac*II were obtained from Promega, and pBluescript KS+ were from Stratagene. Proteinase K, *Apa*I, T3 RNA polymerase, RNase A as well as alkaline-phosphatase-conjugated anti-digoxigenin were from Roche. Horseradish-peroxidase-conjugated goat anti-rabbit antibodies (Envision reagent) were obtained from Dako Cytomation (Glostrup, Denmark) and NovaRed was from Vector Laboratories (Burlingname, CA, U.S.A.). PMA and α-cyano-4-hydroxycinnamic acid were purchased from Sigma.

Tissue samples

In wound healing experiments 6–8-week-old C57BL/6J mice were anaesthetized before full-thickness 20-mm-long incisional skin wounds were made mid-dorsally. Tissue was removed at day 5 or day 7 post wounding. Sections were cut perpendicular to the longitudinal direction of the wounds. Formalin-fixed and paraffin-embedded samples from the periphery of chronic human wounds were kindly provided by Dr E. Balslev from Dept. of Pathology, Dermatology, and Orthopaedics at Bispebjerg Hospital, Copenhagen, Denmark. Samples were collected and assessed in accordance with Danish ethical laws.

The day before induction of PMA-induced hyperproliferation of keratinocytes *in vivo*, the backs of 8–10-week-old female BALB/c mice were shaved. Hyperproliferation was induced by topical application of 6.25 μg of PMA in 200 μl of acetone, covering the shaved area (approx. 3 cm^2). Control mice were treated with 200 μl of acetone only. After treatment for 3 to 48 h the mice were anaesthetized and skin was removed after perfusion-fixation [12].

Samples of human term placenta were collected as described previously [13]. Isolated amnion and chorion membranes from human term placenta, wounds from C57BL/6J mice, and MCF 7 cells were lysed by incubation of their respective homogenates for 30 min on ice with 1 % (v/v) Triton X-114 in 0.1 M Tris/HCl, pH 8.1 (1.1 mg tissue/ml). Detergent phase separation was induced by incubation of the clarified lysates at 37 °C for 5 min to isolate membrane proteins.

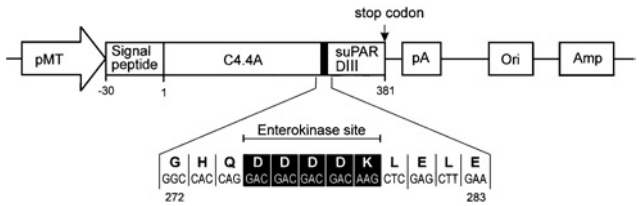

Figure 1 Schematic representation of the expression vector used for C4.4A-uPAR DIII production

The sequence inserted in the expression cassette comprises the original signal sequence for human C4.4A followed by residues 1–274 of human C4.4A (thus omitting the C-terminal signal sequence for GPI-anchoring) fused to residues 182–283 of human uPAR domain III (as affinity tag) via a specific enterokinase cleavage site (DDDDK). PMT, metallothionein promoter; pA, SV40 late polyadenylation signal; Ori, ColE1 origin of replication and, Amp, ampicillin resistance gene.

Design, construction and expression of a soluble C4.4A-uPAR Domain III (DIII) fusion protein

To enable purification and detection of human C4.4A, we constructed a secreted hybrid protein denoted C4.4A-uPAR DIII, comprising residues 1–274 from human C4.4A [3] fused to DIII (residues 182–283) of human uPAR [14]. The linker region between the two proteins also included a cleavage site for enterokinase resulting in a 381-residue-long secreted fusion protein (Figure 1). This construct was inserted into the expression vector pMT/V5-His and co-transfected with the selection vector pCoHygro into *Drosophila melanogaster* Schneider 2 cells (S2 cells), employing CellFectin according to the manufacturer's recommendations. Constitutive secretion of C4.4A-suPAR DIII by these stably transfected S2 cells was accomplished by growth in Drosophila-SFM supplemented with 0.5 mM $CuSO_4$ for 5 days yielding expression levels of approx. 20 mg/l C4.4A-uPAR DIII.

Purification of recombinant C4.4A-uPAR DIII and C4.4A

The fusion protein C4.4A-uPAR DIII was purified from the conditioned media of stably transfected S2 cells by immunoaffinity chromatography using an immobilized monoclonal anti-uPAR antibody (clone R2), which recognizes an epitope on uPAR domain III [11]. Prior to this chromatography, the conditioned medium was clarified by filtration (0.8 μm) after addition of 0.1 volume of 1 M Tris/HCl, pH 8.0 containing 200 mM EDTA and, 0.005 volume of 200 mM PMSF in DMSO.

To remove the affinity tag composed of uPAR DIII, the purified fusion protein C4.4A-uPAR DIII (1 mg/ml) was dissolved in PBS and incubated with enterokinase (10 units/ml) for 16 h at 22 °C. This digest was subsequently loaded onto an affinity column containing immobilized R2 to absorb the liberated uPAR DIII as well as uncleaved C4.4A-uPAR DIII. Pure C4.4A was recovered

in the run-through of the column and was in some cases further purified by reversed-phase HPLC using a Brownlee Aquapore C4 column and a linear gradient (40 min) from 0 % to 70 % (v/v) CH_3CN in 0.1 % (v/v) trifluoroacetic acid.

Production and purification of polyclonal antibodies specific for C4.4A

New Zealand White rabbits were immunized subcutaneously with 20 μg of purified recombinant C4.4A–DIII fusion protein suspended in PBS and Freund's complete adjuvant (The National Serum Institute, Copenhagen, Denmark) followed by weekly subcutaneous injections of 20 μg of C4.4A–DIII in PBS and Freunds incomplete adjuvant. IgG was purified from the immune rabbit serum by protein G affinity chromatography using GammaBind plus Sepharose™, and reactivity towards human uPAR DIII (the affinity tag) was removed by adsorption on a column with immobilized recombinant human suPAR (soluble uPA receptor). This preparation of polyclonal antibodies recognizes native as well as reduced and alkylated human C4.4A, whereas no reactivity towards human uPAR could be detected by immunoblotting (results not shown).

Detection of C4.4A by lectin or immunoblotting

After separation by SDS/PAGE the proteins were transferred to a PVDF membrane (Millipore, Bedford, MA, U.S.A.) by electroblotting at pH 11 using 10 mM Caps [3-(cyclohexylamino)propane-1-sulphonic acid] and 10–30 % (v/v) methanol as transfer buffer [15]. For immunodetection of C4.4A the PVDF membrane was incubated with 2.5 μg/ml of the anti-C4.4A polyclonal rabbit antibodies described above. Blocking, washing and incubation with an alkaline phosphatase-conjugated goat anti-rabbit antibody, as well as development with chemiluminescent substrate, were performed according to the manufacturer's instructions for WesternBreeze™. For carbohydrate detection by lectins the PVDF-membrane was blocked with 2 % (v/v) Tween 20 before incubation with the digoxigenin-labelled lectins AAA, PNA or ConA (5 μg/ml) in 10 mM Tris/HCl, pH 8.0, 150 mM NaCl, 0.05 % (v/v) Tween 20. These lectin blots were developed by incubation with alkaline phosphatase-conjugated anti-digoxigenin (0.4 unit/ml) and visualized by the chemiluminescent substrate as described for the immunoblots.

Enzymic deglycosylation and PI-PLC treatment of C4.4A

To facilitate enzymic hydrolysis of N- and O-linked carbohydrates, purified recombinant C4.4A was reduced by boiling for 2 min in 0.5 M Tris/HCl, pH 8.0, containing 6 M guanidinium chloride, 25 mM EDTA and 50 mM DTT. Generated thiol groups were subsequently alkylated by addition of 0.1 volume of 1 M iodoacetamide. Following a 3-fold dilution in water, these samples were incubated for 16 h at 22 °C with N-glycanase (300 units/ml) and/or O-glycosidase (125×10^{-3} units/ml) before they were analysed by SDS/PAGE. Samples to be analysed by MALDI–TOF-MS (matrix-assisted laser-desorption ionization–time-of-flight mass spectrometry) were boiled for 2 min in 50 mM NaH_2PO_4, pH 6.0, containing 50 % (v/v) ethanol followed by incubation with N-glycanase (100 units/ml) for 16 h at 22 °C to remove N-linked carbohydrates. Deglycosylation of natural C4.4A present in the detergent phases from lysates of human amnion membranes and MCF-7 cells was attempted by a sequential treatment with the exoglycosidases neuraminidase (0.5 unit/ml), β(1-4) galactosidase (0.3 unit/ml) and β-*N*-acetylglucosaminidase (4 units/ml) for 2 h at 37 °C followed by the addition of the endoglycosidases N-glycanase and O-glycosidase before continuing the incubation for 16 h at 22 °C. To cleave GPI-anchors of proteins in amnion and U937 lysates, these were treated with PI-PLC (0.05 units/ml) for 1 h at 37 °C, followed by renewed detergent phase separation in Triton X-114 [7].

Immunohistochemistry

Paraffin-embedded sections (5 μm) were deparaffinized with xylene and hydrated through a series of ethanol/water solutions. Tissue sections of human term placenta or skin wounds were subjected to antigen retrieval by boiling in 10 mM citrate, pH 6.0, for 10 min in a microwave oven, while all sections of mouse incisional skin wounds were treated with proteinase K (10 μg/ml) for 5 min at 37 °C. To block endogenous peroxidase activity, sections were treated with 1 % (v/v) H_2O_2 for 15 min. Sections were washed in 50 mM Tris/HCl, pH 7.6, 150 mM NaCl, containing 0.5 % (v/v) Triton X-100 and incubated overnight at 4 °C with primary antibodies at the following concentrations: polyclonal rabbit IgG against C4.4A and pre-immune rabbit IgG at 2.5 μg/ml, and polyclonal rabbit IgG against mouse uPAR at 10 μg/ml [16]. In some control experiments the anti-C4.4A antibodies were pre-incubated for 30 min with a 5-fold molar excess of purified C4.4A. Goat anti-rabbit IgG (Envision reagent) was used as secondary antibody and the sections were developed with NovaRed for 10 min as specified by the manufacturer. Sections were finally counter-stained with Mayer's haematoxylin for 30 s, dehydrated in ethanol and mounted [17].

In situ hybridization

A nucleotide covering position 313–989 (accession number AJ223603) was obtained by enzymic digestion with *Sac*II and *Apa*I of a plasmid (pT7T3-C4.4A) containing the full-length cDNA of human C4.4A [3], and this fragment was subsequently cloned into pBluescript KS+. Antisense and sense probes were obtained by *in vitro* transcription using ^{35}S-labelled rUTP, T3 and T7 RNA polymerases. *In situ* hybridisation was performed as described previously [17], with the exception that the sections were pretreated by boiling for 12 min in 10 mM citrate, pH 6.0, using a microwave oven.

Amino acid composition, N-terminal protein sequencing and MALDI–TOF-MS analyses

10 μl of an HPLC-purified C4.4A preparation ($A_{280} = 0.147$) was dried by vacuum evaporation and subsequently hydrolysed *in vacuo* for 20 h at 110 °C in 100 μl of 6 M HCl containing 0.05 % (w/v) phenol and 5 μl of 1 % (w/v) 3,3′-dithiodipropionic acid in 0.2 M NaOH. Quantification of the released amino acids was performed on a Waters amino acid analyser equipped with post column *o*-phthaldialdehyde derivatisation [18]. The molar absorption coefficient determined from these experiments for C4.4A is 12 500 $M^{-1}cm^{-1}$.

Reduced and alkylated C4.4A fragments created by limited proteolysis were separated by SDS/PAGE and transferred to PVDF membrane by electroblotting using 10 mM Caps and 10 % (v/v) methanol at pH 11.0. Protein fragments were visualized by Coomassie Brilliant Blue R250 staining and N-terminal protein sequence analysis was performed on PVDF immobilized protein fragments as described previously [19].

N-glycanase-treated samples were loaded on C4 nanoscale reversed-phase columns [20] and eluted with 15 μg/μl α-cyano-4-hydroxycinnamic acid in 70 % (v/v) CH_3CN directly onto a MS target precoated with matrix. MALDI–TOF-MS spectra were recorded on a linear time-of-flight instrument (Voyager, Perseptive Biosystems, MA, U.S.A.). Mass spectra were internally

calibrated using β-lactoglobulin A (18363.3 Da) and pro-uPA (46399.5 Da) as standards.

Interaction analysis by surface plasmon resonance and cell binding

Recombinant C4.4A and uPAR (residues 1–283), both produced in S2 cells, were immobilized on a carboxylated dextran matrix by amine coupling using N-hydroxysuccinimide/N-ethyl-N′-[3-(diethylamino)propyl]carbodiimide [21]. Coupling yields of 1000–3000 resonance units were typically obtained. Real-time biomolecular interaction analyses were recorded by a BIAcore 2000™ (Pharmacia Biosensor, Sweden) at a flow rate of 10 μl min^{-1} at 6 °C using 10 mM Hepes, 150 mM NaCl, 0.005 % (v/v) surfactant P-20 (pH 7.4) supplemented with either 3 mM EDTA or 5 mM $CaCl_2$ and 2 mM $MgCl_2$ as running buffer. The sensor chip was regenerated at the end of each run by two consecutive injections of 0.1 M acetic acid containing 0.5 M NaCl.

Possible interactions between uPA and GPI-anchored C4.4A were tested in cell binding experiments measuring the binding of 20 nM ^{125}I-labelled pro-uPA to MCF 7 cells. 3×10^5 MCF 7 cells/well were seeded in wells and were approx. 90 % confluent after overnight incubation. Cells were pre-incubated with RPMI media containing 0.5 % (v/w) BSA with or without 300 nM monoclonal antibody R3, or 200 nM uPA for 15 min at 4 °C with shaking. 20 nM ^{125}I-labelled pro-uPA was added and incubation was continued at 4 °C for 1 h. Cells were subsequently washed in RPMI media containing 0.5 % (v/w) BSA, lysed with 1 M NaOH for 10 min, and the level of pro-uPA binding was calculated after γ-counting.

RESULTS

Expression and purification of soluble recombinant human C4.4A

To enable an initial biochemical characterization of the human orthologue of rat metastasis-associated C4.4A, which has so far been analysed only by mRNA-related techniques [2–4], we expressed a recombinant soluble form of human C4.4A in S2 cells. As shown in Figure 1 our expression vector encodes a hybrid protein (denoted C4.4A-uPAR DIII) including the first 274 residues of the human C4.4A followed by an enterokinase-specific cleavage site and the third domain of the urokinase receptor, which acts as an affinity tag. This hybrid protein was expressed and secreted in very high yields by the S2 cells. After 5 days of induction, the medium typically contained 20 mg/l of C4.4A-uPAR DIII as assessed by immunoblotting using a monoclonal detecting antibody specific for the uPAR DIII tag (R2) [22] and purified soluble uPAR as standard (results not shown). The secreted fusion protein was purified to homogeneity by immunoaffinity chromatography using the R2 monoclonal anti-uPAR antibody (Figure 2, lanes 2 and 3). Incubation of this purified C4.4A-uPAR DIII with enterokinase led to an efficient cleavage of the introduced linker (> 90 %; Figure 2, lane 4). The liberated C4.4A was subsequently purified by a second immunoaffinity chromatography from which it was recovered in the run-through of the R2 column (Figure 2, lane 5). As judged by SDS/PAGE the main component in this preparation is intact soluble C4.4A. The electrophoretic mobility of this C4.4A appears relatively broad ($M_r \sim 50000$) which is indicative of a high level of endogenous glycosylation (Figure 2, lane 5). Also present, but much less abundant, is a smaller component ($M_r \sim 35000$) that is formed during the incubation with enterokinase and migrates as a doublet during SDS/PAGE (Figure 2, lanes 4 and 5). As shown below, this component is likely to represent an N-terminal fragment of C4.4A, which spans the first approx. 200 residues and we have termed this fragment C4.4A′.

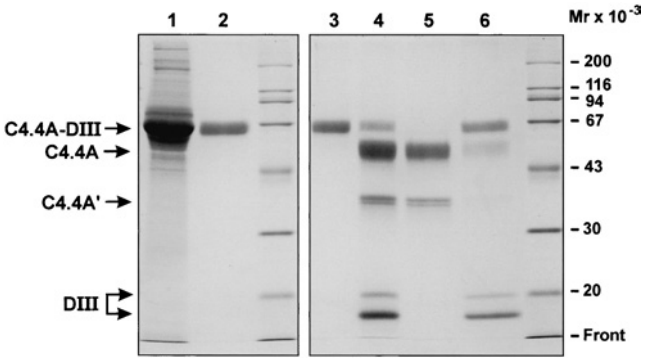

Figure 2 Affinity purification of recombinant C4.4A-uPAR DIII and C4.4A after enterokinase cleavage

The fusion protein C4.4A-uPAR DIII was purified from the conditioned media of stably transfected S2 cells (lane 1) by R2-immunoaffinity chromatography and acid elution (lanes 2 and 3). After enterokinase cleavage of the fusion protein (lane 4) the liberated C4.4A was recovered from the run-through of an R2-column (lane 5), which retained the uncleaved fusion protein as well as uPAR DIII (lane 6). Shown is a Coomassie Brilliant Blue G-250-stained polyacrylamide gel (12 %) after SDS/PAGE of reduced and alkylated samples (5 μl medium containing approx. 0.1 μg of C4.4A-uPAR DIII was applied in lane 1, whereas lanes 2–6 each contained 1–3 μg of purified protein). C4.4A′ is a degradation product of C4.4A comprising its two Ly-6/uPAR/α-neurotoxin-like domains. DIII, uPAR DIII.

Post-translational modification of human C4.4A by extensive glycosylation

The amino acid composition determined for purified recombinant C4.4A after acid hydrolysis is in accordance with its cDNA-derived composition and reveals the presence of approx. 15 residues of both glucosamine and galactosamine in C4.4A (Table 1), which most likely originate from the acid hydrolysis of N- and O-linked carbohydrates respectively. To substantiate this finding further, we tested the reactivity of C4.4A with various lectins, recognizing epitopes predominantly present in either O- or N-linked carbohydrates (PNA versus Con A and AAA). As shown in Figure 3, intact recombinant C4.4A is recognized by all three lectins in patterns that are sensitive to treatment with either O-glycosidase (PNA) or N-glycanase (Con A and PNA). The presence of O-linked carbohydrates in C4.4A is clearly revealed by its specific reactivity with the lectin PNA (Figure 3B, lane 1). This interaction is abolished by pretreatment of C4.4A with O-glycanase (Figure 3B, lanes 3 and 4), but not with N-glycanase (Figure 3B, lane 2). The distinct shift in electrophoretic mobility of C4.4A by the latter treatment is also indicative of the removal of some N-linked carbohydrates. Direct evidence for the presence of N-linked carbohydrates in intact C4.4A is provided by its specific recognition by the lectins ConA and AAA in reactions that are sensitive to treatment with N-glycanase (Figures 3C and 3D, lanes 1 and 2) but not with O-glycanase (lanes 3 in Figures 3C and 3D). Furthermore, from these experiments it is noticeable that the aforementioned truncated fragment C4.4A′ is detected by Con A and AAA but not by PNA and this recognition is sensitive to N-glycanase treatment only (Figures 3B–3D, lanes 1–3). Collectively these experiments demonstrate that C4.4A is modified by both N- and O-linked carbohydrates attached in a polarized orientation with the O-linked carbohydrates, being localized in proximity to the C-terminus (i.e. absent from C4.4A′).

To establish whether human C4.4A, like its rat orthologue [1], is a glycolipid-anchored membrane protein *in vivo*, we tested lysates from human term placenta for the presence of C4.4A protein by detergent-phase separation followed by immunoblotting. Term

Table 1 Amino acid composition of purified recombinant C4.4A after enterokinase cleavage, monoclonal R2-affinity chromatography and reversed-phase HPLC

The composition is calculated from a single amino acid analysis after hydrolysis for 20 h assuming that the protein sequence comprises 279 residues.

Amino acid	Determined after acid hydrolysis (mol amino acid/mol uPA)	Residues/uPAR as predicted from cDNA of C4.4A (residues 1–274 + DDDDK)
Asx	29.1	28
Thr	24.4*	25
Ser	24.8*	24
Glx	24.7	24
Pro	23.1	24
Gly	26.2	26
Ala	20.2	21
Cys†	17.8†	18
Val	21.1	23
Met	2.3	2
Ile	2.8	3
Leu	20.0	19
Tyr	5.8	6
Phe	6.1	6
His	5.4	5
Lys	10.2	10
Arg	14.9	15
Trp	NA	0
GlcNAc	15.2*	12‡
GalNAc	15.2*	15‡

* These values are corrected for decomposition occurring during hydrolysis assuming an average loss of 5 % for Thr, 10 % for Ser and 50 % for both *N*-acetylglucosamine and *N*-acetylgalactosamine.

† Cysteine was derivatized during hydrolysis in the presence of 3,3′-dithiodipropionic acid and was quantified as the mixed disulphide [18].

‡ A rough estimate of the carbohydrate content was made assuming that each *N*-linked glycosylation sequenon (*N*-X-T/S) carried a primitive glycosylation containing 2 *N*-acetylglycosamines, whereas the *O*-linked glycosylation sites predicted by NetOGlyc 2.0 [26] are assumed to contain a single *N*-acetylgalactosamine [36]. NA; not applicable.

placenta was chosen for these studies because this organ contains a high level of C4.4A mRNA according to studies using Northern blotting [3]. Total lysates of isolated amnion membranes did indeed contain a distinct component reactive with the polyclonal anti-C4.4A antibodies, while this component was absent from chorion lysates (Figure 4, left-hand panel). The difference in electrophoretic mobility observed between the placental C4.4A (M_r ~90000) and our recombinant, soluble C4.4A (M_r ~50000) is likely to reflect differences in maturation and complexity of N- and O-linked carbohydrates. This interpretation is further substantiated by the observation that a combined treatment with N- and O-glycosidases leads to widely different shifts in the electrophoretic mobility of placental C4.4A compared with S2-produced C4.4A, which translate into size reductions of 35000 Da for placental C4.4A *versus* 5000 Da for the recombinant protein (results not shown).

The presence of a glycosyl-phosphatidylinositol moiety in placental C4.4A was subsequently probed by its partitioning properties during temperature-induced detergent-phase separation in Triton X-114. The selective detergent-phase partitioning observed for native placental C4.4A (Figure 4, middle panel, lanes 2 and 3) is thus shifted towards the aqueous phase upon treatment with PI-PLC that specifically removes the hydrophobic lipid moieties of glycolipid anchors (Figure 4, middle panel lanes 4 and 5). Also included as a positive control is a parallel analysis of the detergent-phase partitioning properties of the glycolipid-anchored uPAR from U937 cells [7]. The incomplete conversion of the hydrophobic properties observed for both C4.4A and uPAR after PI-PLC treatment may reflect an additional acylation of the glycolipid-anchor in a fraction of these molecules that renders them resistant to PI-PLC [7].

Probing recombinant C4.4A by limited proteolysis

The susceptibility of recombinant C4.4A to proteolysis under native conditions was subsequently probed by incubation with 2-fold dilutions of chymotrypsin and trypsin. The observed resistance towards proteolysis over a wide range of protease concentrations is in favour of an overall folded state of the recombinant C4.4A (Figure 5A). However, both proteases did generate with great efficiency a single fragment, which migrates as a doublet during SDS/PAGE (M_r ~35000; Figure 5A) and is indistinguishable from the C4.4A′ generated during enterokinase cleavage of the fusion protein (Figure 2, lane 4). Accordingly this fragment showed no reactivity with the lectin PNA demonstrating the absence of O-linked carbohydrates (results not shown). Studies by MS (Table 2) reveal that these C4.4A fragments were

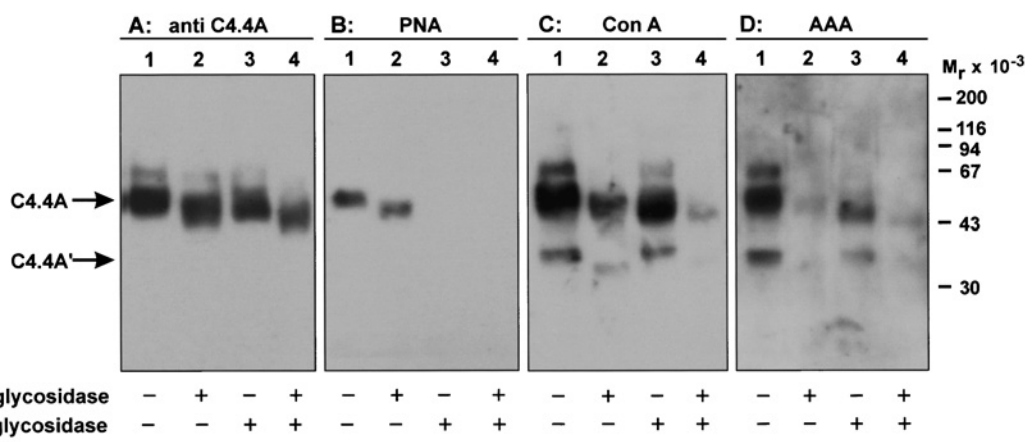

Figure 3 Demonstration of N- and O-linked glycosylation in recombinant C4.4A

Purified C4.4A (25 ng) was analysed by SDS/PAGE and transferred to PVDF-membrane by electroblotting before (lanes 1) and after (lanes 2) treatment with N-glycanase, O-glycosidase (lanes 3) or both enzymes in combination (lanes 4). The blots were incubated with either polyclonal antibodies specific for C4.4A (2.5 μg/ml; panel **A**) or the lectins (5 μg/ml): PNA [recognizing Gal-β(1,3)-GalNAc; panel **B**]; Con A (recognizing α-mannose, panel **C**); and AAA (recognizing α-fucose; panel **D**). The C4.4A samples were reduced and alkylated prior to SDS/PAGE.

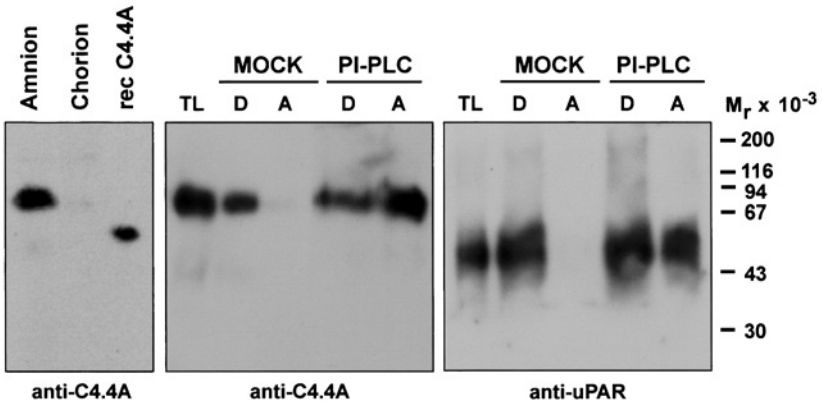

Figure 4 Detergent-phase separation of placental C4.4A

Left-hand panel shows an immunoblotting analysis for C4.4A in total lysates of amnion and chorion membranes isolated from human term placenta. Also included is purified recombinant C4.4A as positive control (10 ng). The middle panel reveals the detergent-phase partitioning properties of amnion C4.4A before and after treatment with PI-PLC (5 units/ml) and the right-hand panel shows the similar properties tested for human uPAR in lysates from PMA-treated U937 cells. Unreduced samples were analysed by SDS/PAGE, electroblotted onto PVDF-membranes in the presence of 30 % (v/v) methanol and developed with either the polyclonal anti-C4.4A antibodies (2.5 μg/ml) or a monoclonal anti-uPAR antibody R2 (2.5 μg/ml). TL, total lysates; D, detergent phase; A, aqueous phase.

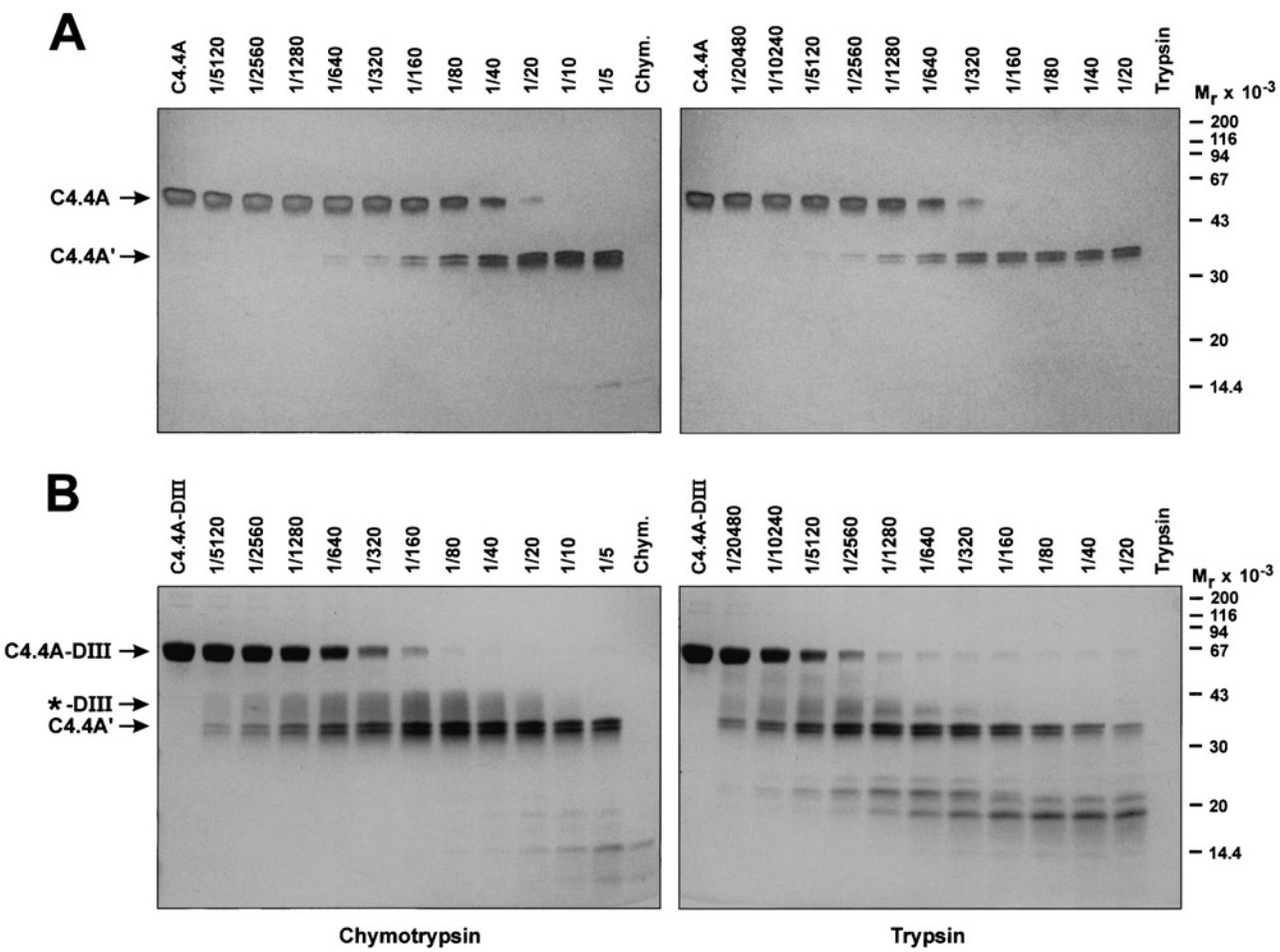

Figure 5 Limited proteolysis of recombinant C4.4A and C4.4A-uPAR DIII by trypsin and chymotrypsin

Purified C4.4A (0.2 μg; panel **A**) and C4.4A-uPAR DIII (2.5 μg; panel **B**) were incubated with either trypsin or chymotrypsin in PBS at the indicated enzyme substrate ratio (w/w) for 2 h at 37 °C before they were analysed by SDS/PAGE after reduction and alkylation. Polyacrylamide gels (12 %) were developed by either silver staining (panel **A**) or Coomassie Brilliant Blue G-250 staining (panel **B**). C4.4A-DIII, C4.4A-uPAR DIII; chym., chymotrypsin.

Table 2 Identification of tryptic and chymotryptic fragments of C4.4A-DIII by MS and N-terminal protein sequencing

C4.4A fragments correspond to those shown in Figure 5(B) and are designated accordingly. MALDI–TOF-MS spectra were recorded for N-glycanase treated samples and the calculated average masses are therefore corrected for six asparagine to aspartic acid conversions induced by the catalytic mechanism of N-glycanase. The spectrum for C4.4A′ chymotrypsin contained two fragments having comparable peak intensities. Protein sequence analysis was performed on PVDF-immobilized proteins. The *-DIII trypsin fragment contained one dominating sequence, whereas the fragment *-DIII chymotrypsin yielded a mixed sequence, which could be accounted for by the shown sequences.

C4.4A-DIII fragment	Measured MH^+ (Da)	Calculated MH^+ (Da)	Identity
C4.4A′ trypsin	21 442.9	21 453.0	1–204
C4.4A′ chymotrypsin	20 982.4	20 965.5	1–200
	21 101.5	21 112.7	1–201

C4.4A-DIII fragment	Protein sequence	Identity
C4.4A sequence	. . . RNKTYFSPRIPPLVRLPPPEPT . . .	196–216
*-DIII trypsin	. . . IPPLVRLPP . . .	205–213
*-DIII chymotrypsin	. . . FSPRIPPLV . . .	201–209
	. . . SPRIPPLVR . . .	202–210

generated by a single cleavage occurring at Arg^{204} (by trypsin) or Tyr^{200}/Phe^{201} (by chymotrypsin). The size heterogeneity of the generated C4.4A′ was eliminated by N-glycanase treatment, thus demonstrating that it is caused by an incomplete glycosylation efficiency (results not shown).

Limited proteolysis of the fusion protein, C4.4A-uPAR DIII, by chymotrypsin or trypsin generates, in addition to the expected C4.4A′, a second fragment having a less well-defined electrophoretic mobility (M_r ~35 000–45 000). This fragment, marked as *-DIII in Figure 5(B), is reactive with the lectin PNA as well as the monoclonal anti-uPAR antibody R2 (results not shown), demonstrating that it covers the C-terminal region of C4.4A linked to uPAR DIII. Protein sequence determinations by Edman degradation (Table 2) identified the scissile peptide bonds in C4.4A as Arg^{204}-Ile^{205} for trypsin, and Tyr^{200}-Phe^{201} and Phe^{201}-Ser^{202} for chymotrypsin. The corresponding C-terminal fragment is not observed in Figure 5(A) because of the inherent difficulties of fixing and staining small highly glycosylated polypeptides.

Probing the interaction between C4.4A and uPA using purified human components

With a view to the structural homology between C4.4A and uPAR, it seemed reasonable to test whether some of the established ligands for uPAR also interact with C4.4A, thus raising the possibility of a functional overlap between the two. To address this question we immobilized purified recombinant C4.4A and uPAR on a biosensor chip and explored their binding properties towards a selection of purified proteins by surface plasmon resonance. The outcome of this brief survey is shown in Table 3. Using this experimental set up we find no evidence for any interaction between recombinant C4.4A and either uPA, vitronectin, uPAR or C4.4A itself.

To examine possible interactions between GPI-anchored human C4.4A on the cell surface and human uPA, as reported previously by Zöller and co-workers for the rat components [1], we tested various human cell lines for the expression of C4.4A using the purified preparation of polyclonal anti-C4.4A antibodies. A significant expression of C4.4A was observed for the breast cancer-derived cell line MCF 7 (Figure 6I, lane 3), which has been shown previously to possess low levels of uPAR expression [23].

Table 3 Binding properties of C4.4A and uPAR towards selected purified proteins as assessed by surface plasmon resonance

Protein interactions were measured by surface plasmon resonance using a BIAcore 2000 with recombinant C4.4A (1345 RU) and suPAR (2887 RU) immobilized on the sensor chip. Shown are the binding levels in resonance units (RU) obtained after a contact time of 10 min at a flow rate of 10 μl/min at 6 °C. Sensorgrams were background subtracted using a non-protein coupled flow cell analysed in parallel.

Analyte	C4.4A (RU)	uPAR (RU)
pro-uPA (200 nM)	< 5	800
suPAR (200 nM)	< 5	< 5
suPAR • pro-uPA (200 nM)	10	< 5
C4.4A (200 nM)	< 5	< 5
Vitronectin (200 nM)	< 5	230
Lectin PNA (1.7 μM)*	410	20
Anti-C4.4A (300 nM)*	280	< 5

* Measurements obtained in running buffer where EDTA was replaced by 5 mM $CaCl_2$ and 2 mM $MgCl_2$.

In cell binding experiments we observed a low capacity binding for 20 nM ^{125}I-labelled pro-uPA to MCF 7 cells, a property which was abolished by pre-incubation with a monoclonal anti-uPAR antibody (R3), which competes with the uPA-uPAR interaction (results not shown). The observed binding of ^{125}I-labelled pro-uPA to MCF 7 cells is therefore entirely mediated by uPAR.

Immunohistochemical localization of C4.4A in term placenta and skin

Immunohistochemical studies of human term placenta with the preparation of anti-C4.4A polyclonal antibodies showed (as expected from previous studies by Northern blotting [2,3]) a pronounced immunoreactivity for C4.4A. This reactivity was confined to the amniotic membrane (Figures 6A and 6B), in agreement with the previously discussed data obtained by immunoblotting of lysates from isolated chorion and amnion membranes (see Figure 4, left-hand panel). The corresponding absorption control using purified recombinant C4.4A showed no staining, supporting the specificity of the immune reaction (Figure 6C).

A distinct membrane-associated C4.4A staining was also observed on suprabasal keratinocytes in chronic human wounds, whereas the basal keratinocytes were negative (Figure 6D). Again, the corresponding absorption control showed no staining (results not shown). This expression pattern was further supported by *in situ* hybridization of adjacent sections, since the corresponding cell populations revealed specific hybridization signals with a C4.4A antisense probe (Figure 6E), while no signal was obtained with the sense probe (Figure 6F).

To facilitate future investigations of C4.4A expression in various experimental animal model systems the cross-reactivity of the purified polyclonal anti-C4.4A antibodies with murine C4.4A was explored using day 5 murine incisional wounds (Figures 6G–6I). Only a single component, with an electrophoretic mobility corresponding to human C4.4A, is recognized by the polyclonal anti-C4.4A antibodies in total lysates from murine wounds, which demonstrates the specificity of this cross-reactivity with murine C4.4A (Figure 6I, compare lanes 1 and 3). Furthermore, the pronounced immunoreactivity observed in the mouse skin after wounding (Figure 6G) is abolished in the appropriate absorption control with human C4.4A (Figure 6H).

Having demonstrated the specificity of the immunoreactivity with murine C4.4A, we next evaluated C4.4A expression during healing of incisional wounds in mouse skin. At the wound edge,

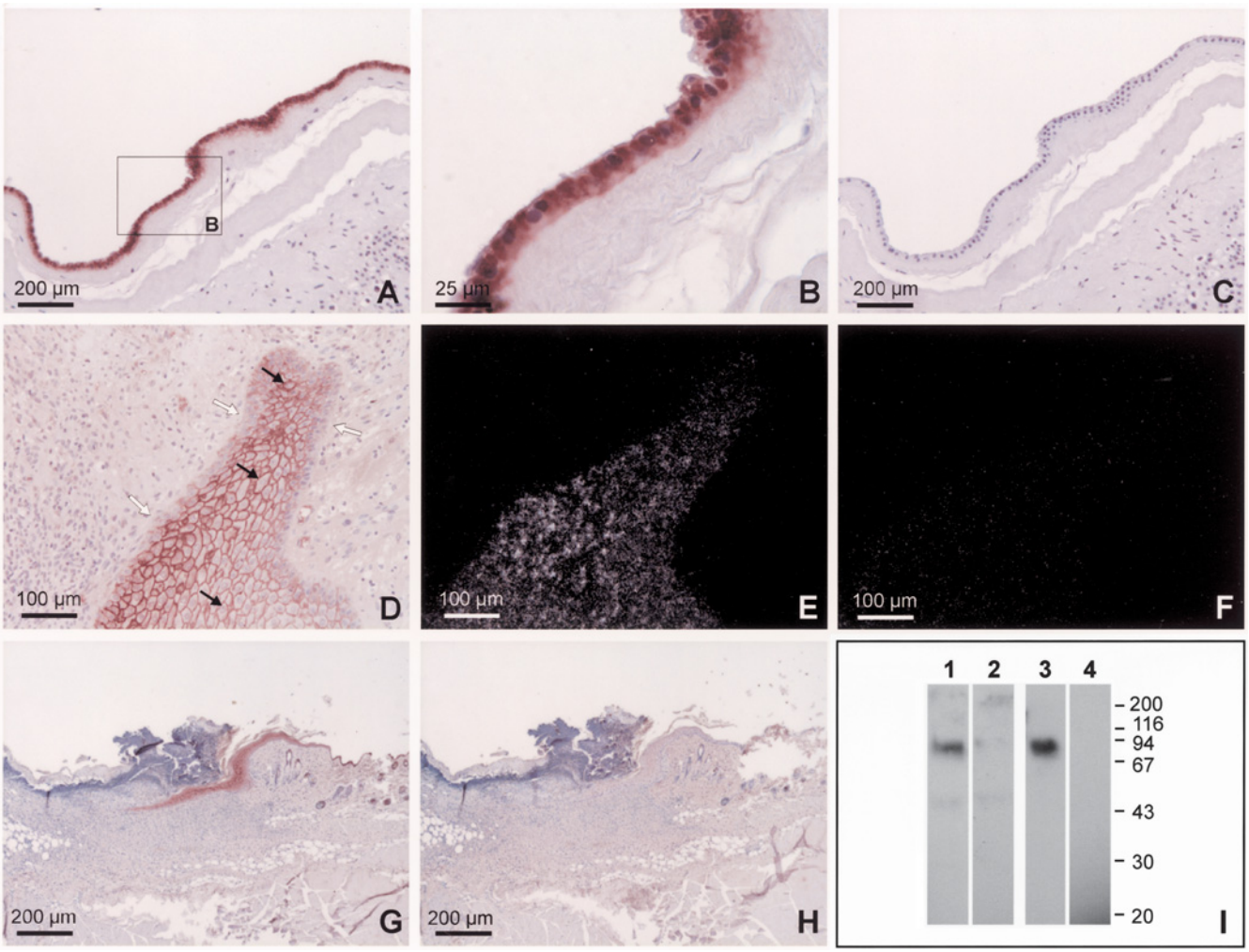

Figure 6 C4.4A expression in term placenta and skin wounds determined by immunohistochemistry, *in situ* hybridisation, and immunoblotting

Shown are serial sections of human term placenta (**A**–**C**), human wounds from chronic leg ulcers (**D**–**F**) and murine skin day 5 post incisional wounding (**G**–**H**). For immunohistochemistry, sections were incubated with 2.5 μg/ml of the polyclonal antibodies against C4.4A, either alone (**A**, **B**, **D**, **G**), or after preincubation with a 5-fold molar excess of purified C4.4A antigen (**C**, **H**). For *in situ* hybridisation sections were either incubated with ^{35}S-labelled antisense (**E**) or sense (**F**) probes for C4.4A mRNA; here shown with darkfield illumination. The white arrows indicate the C4.4A negative basal keratinocytes of human skin wounds (**D**), while the black arrows indicate the C4.4A positive cells (**D**). Immunoblots (**I**) of total lysates from mouse wounds (lanes 1 and 2) and the human breast carcinoma cell line MCF 7 (lanes 3 and 4) were incubated with 2.5 μg/ml polyclonal anti-C4.4A antibodies either alone (lanes 1 and 3) or after preincubation with a 5-fold molar excess of purified C4.4A antigen (lanes 2 and 4).

where basal keratinocytes are undergoing active proliferation and differentiation, C4.4A staining is confined to the suprabasal cells presenting a moderately increased expression level (Figure 7B) compared with the epithelial layers of the normal homeostatic skin (Figure 7A). The upregulation of C4.4A expression appears to increase along the sheet of migrating keratinocytes, resulting in a prominent staining of the keratinocytes located at the end of the wound tongue (Figure 7C). The basal keratinocytes are negative throughout the wound (Figures 7A–7C, white arrows). Intriguingly, C4.4A expression was almost absent from the few keratinocytes forming the very outermost tip of the tongue (Figure 7C).

To further investigate C4.4A expression during abnormal conditions in the skin, immunohistochemical staining of PMA-induced hyperplasia of mouse skin was performed. Only 3 h after PMA application an increase in expression of C4.4A is seen in the suprabasal keratinocytes (Figure 8B), compared with the control skin treated with solvent (Figure 8A). This high level of C4.4A expression in the hyperplasic suprabasal layers is sustained for more than 48 h (Figures 8B–8E), while the basal keratinocytes remain negative (Figures 8A–8E). Epidermal cells of hair follicles also acquire an increased C4.4A expression as a result of the PMA stimulation (Figures 8A–8E, arrowheads). To compare the expression pattern of the homologous proteins C4.4A and uPAR, adjacent sections were probed with polyclonal anti-uPAR and anti-C4.4A antibodies 9 h after PMA stimulation (Figure 8F). A comparison of Figures 8(C) and 8(F) reveal an almost complementary expression pattern of these proteins. No uPAR can thus be detected in either the hyperproliferative keratinocytes or the epidermal cells of hair follicles. In contrast, numerous scattered cells in the dermis are clearly uPAR positive and C4.4A negative. These cells probably represent infiltrating polymorphonuclear leucocytes and macrophages.

DISCUSSION

Human and rat C4.4A have been recently identified by two unrelated screening methods designed to select proteins that are

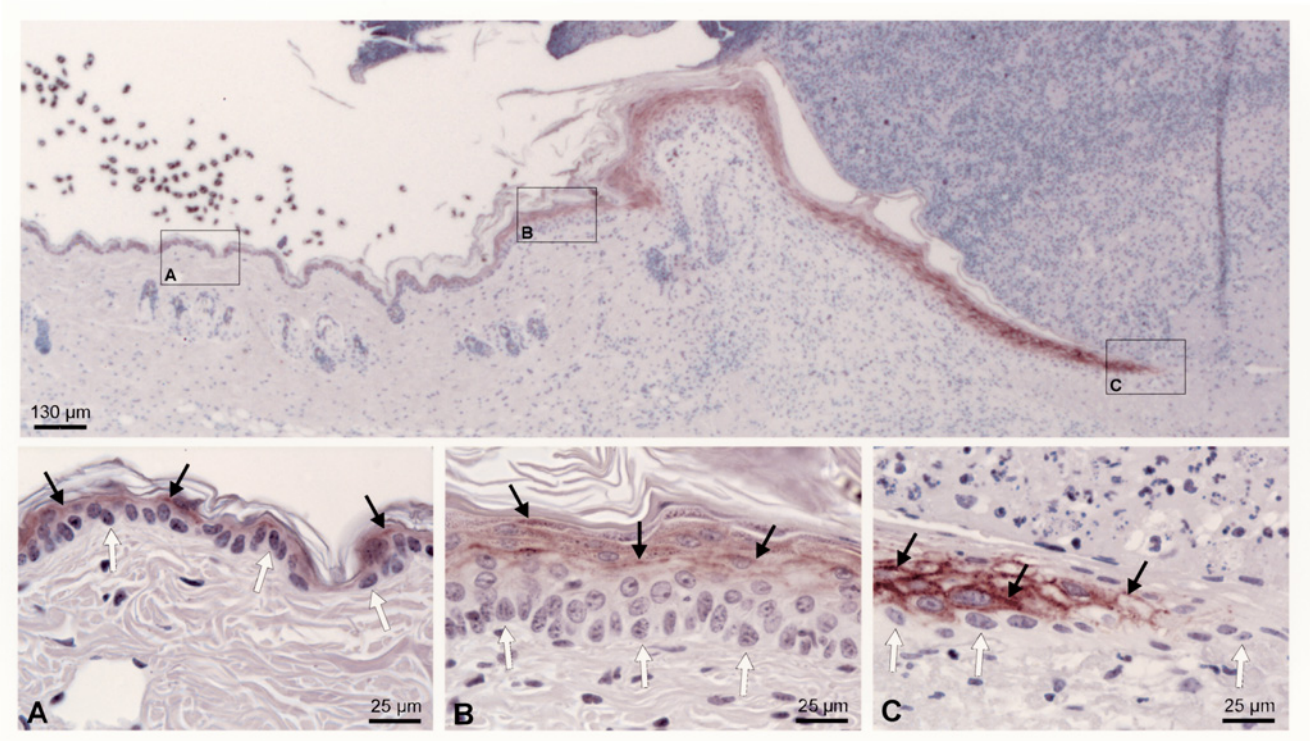

Figure 7 Upregulation of C4.4A in migrating murine keratinocytes during wound healing

A section of a 7-day-old murine incisional wound was incubated with 2.5 μg/ml of polyclonal anti-C4.4A antibodies followed by immunoperoxidase staining using NovaRed chromogene. An overview of the wound is shown in the upper panel at low magnification, while the insets are shown in the lower panels at higher magnification (see scale bars). The single layer epithelium adjacent to the wound (**A**), the proliferating keratinocytes at the wound edge (**B**), and the tip of the migrating keratinocytes closing the wound (**C**) are shown. Note the intense C4.4A staining of the migrating keratinocytes in (**C**) compared with the normal epidermis in (**A**) and the proliferating keratinocytes in (**B**). The white arrows indicate the C4.4A-negative basal keratinocytes, while the black arrows indicate the C4.4A-positive cells. As in Figure 6, immunoreactivity of this 7-day-old wound was abolished upon preincubation with recombinant C4.4A.

differentially up-regulated during conditions assumed to mimic malignant progression of cancer [1,2]. Interestingly the cDNA-derived sequences covering the first 191 residues of these C4.4A proteins comply with the consensus rules established for Ly-6/uPAR/α-neurotoxin protein modules [5,6]. The extracellular region of C4.4A is therefore assumed to include two such consecutive Ly-6/uPAR/α-neurotoxin modules followed by an unrelated C-terminal region, which is rich in serine, threonine, and proline (STP-rich region) and which terminates in a GPI membrane anchor (as illustrated in Figure 9A). Collectively these properties render C4.4A a close structural homologue of the urokinase receptor despite the low sequence identity that is observed for the pairwise homologous domains (approx. 25%).

The structural properties that are shared between uPAR and C4.4A include their attachment to the cell membrane by a glycolipid anchor (as demonstrated in Figure 4 and [1,7]) and their organization as multidomain proteins, where C4.4A contains two Ly-6/uPAR/α-neurotoxin domains compared with the three present in uPAR (see Figure 9 and [5,6]). One of the unique structural hallmarks for uPAR domain I is, furthermore, replicated in the N-terminal domain I of C4.4A as these two modules are the only members of the Ly-6/uPAR/α-neurotoxin protein-domain family to lack the seventh and eighth cysteine residues [5,11]. The importance of this common feature is further emphasized by the observation that this particular disulphide bond, connecting these two cysteines, appears to be critically involved in stabilizing the three-finger fold of the single domain members [24,25]. Additional evidence for the evolutionary relationship between these proteins is provided by the chromosomal location and organization of the genes encoding human C4.4A and uPAR, since both genes are located on chromosome 19q13.2 [3,8] only 180 kb apart. In addition, the regions in both genes that encode the Ly-6/uPAR/α-neurotoxin modules comprise separate exon sets having their internal phase-1 introns located at sites corresponding to surface exposed loops of the generalized three-finger fold of the module, Figures 9(A) and 9(B) [6].

The present biochemical characterization of purified recombinant C4.4A has, however, revealed two structural properties that are not shared with uPAR. C4.4A and uPAR are both modified extensively by N-linked carbohydrates [1,21], but only C4.4A is modified by O-linked glycosylation. Despite the fact that a previous study on recombinant rat C4.4A [1] failed to demonstrate any post-translational modification by O-linked carbohydrates using an inhibitor of this glycosylation pathway, we now find that recombinant human C4.4A, expressed by S2 cells, does indeed contain a substantial amount of O-linked carbohydrates. Combining enzymic deglycosylation and lectin blotting we demonstrate (see Figure 3) that the modification of human C4.4A with O-linked carbohydrate occurs in the C-terminal STP-rich region, which has no structural counterpart in uPAR (Figure 9). Concordant with this, amino acid composition analysis estimates a content of 15 *N*-acetylgalactosamine residues in purified C4.4A, which agrees nicely with the number of putative O-linked glycosylation sites in the STP-rich domain that was predicted from the cDNA derived sequence by a computer algorithm [26] (Figure 9). The

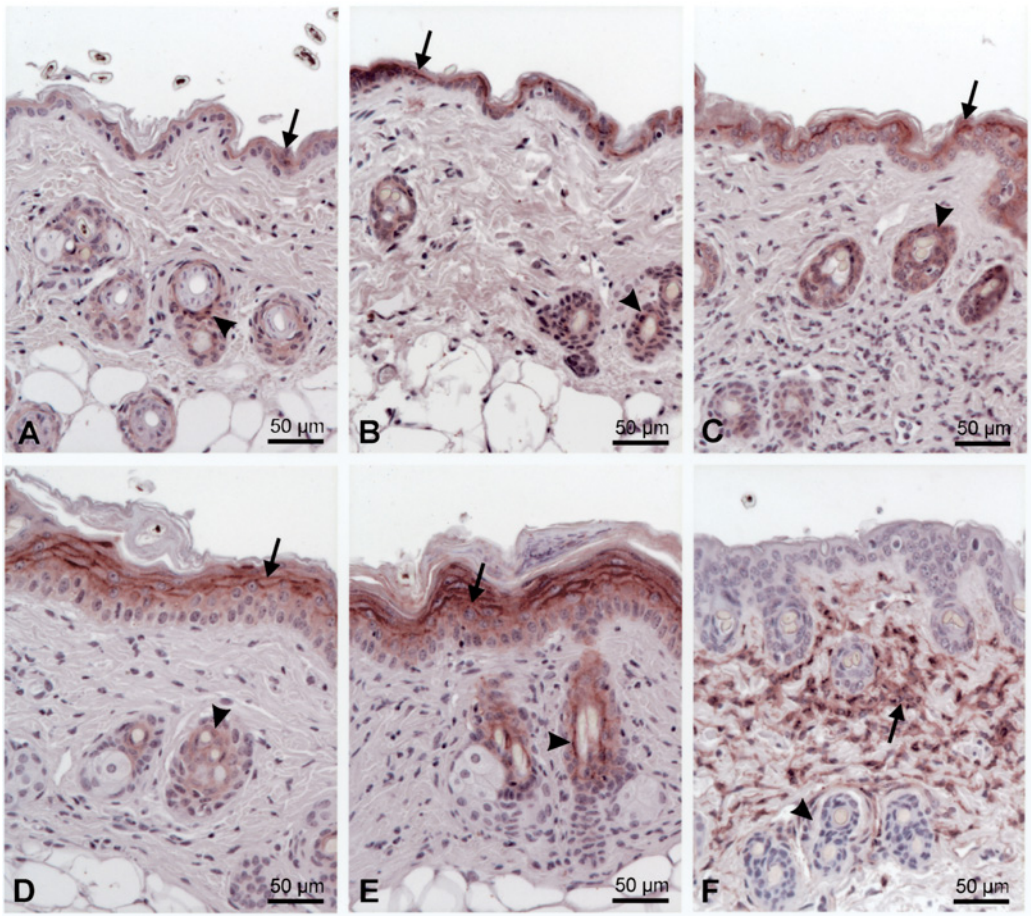

Figure 8 Induction of C4.4A in mouse epidermis after PMA treatment

Sections of skin obtained from mice treated with solvent alone for 48 h (**A**) or with a single dose of PMA for 3 h (**B**), 9 h (**C** and **F**), 24 h (**D**), and 48 h (**E**) were incubated with 2.5 μg/ml polyclonal anti-C4.4A antibodies (**A**–**E**), or with 10 μg/ml polyclonal anti-uPAR antibodies (**F**) followed by immunoperoxidase staining using NovaRed chromogene. Black arrows indicate C4.4A-positive cells, and arrowheads highlight hair follicles.

functional consequences for C4.4A of this modification remain speculative, but generally the presence of domains with multiple O-linked carbohydrates tend to confer an elongated structure to the polypeptide backbone [27], and the STP-rich domain of C4.4A may therefore serve to project the Ly-6/uPAR/α-neurotoxin domains of C4.4A above the cell membrane. Interestingly, these two specific domains of C4.4A have recently been suggested to form the minimal functional binding site for two human proteins, AG-2 and AG-3, as delineated by yeast two-hybrid cloning [28]. These two proteins have not yet been assigned a function, but they are frequently expressed by the tumour cells in ductal mammary carcinomas [28].

Another major difference between recombinant C4.4A and uPAR is revealed by limited proteolysis using trypsin and chymotrypsin. Although both proteins are relatively resistant to proteolytic degradation they do, nevertheless, possess specific inter-domain linker regions that are highly susceptible to enzymic hydrolysis. In human uPAR, this protease sensitive region is localized between uPAR domains I and II (residues 83–89), whereas in C4.4A it is situated between domain II and the STP-rich region (see Figures 5 and 9). Interestingly this inter-domain cleavage has a significant impact on uPAR function, since it abrogates the high affinity for both uPA [29] and vitronectin [30]. Furthermore, it has been recently suggested that this particular cleavage also exposes a putatively cryptic interaction site on uPAR for a chemotactic G-protein-coupled receptor [31]. Whether a similar inter-domain cleavage of C4.4A, followed by shedding of domains I + II, actually occurs *in vivo*, and its functional implications, is unknown presently. It would, however, be interesting to investigate whether disease progression of, for example, bladder cancer is correlated with an increased level of such soluble C4.4A derivatives in urine and plasma from these patients since studies by *in situ* hybridisation suggest that C4.4A expression is up-regulated during progression of urothelial cancer [2]. Such correlations between malignancies and plasma levels of soluble uPAR are already well established for several types of human cancer [32,33].

It has been proposed previously that the structural relationship between uPAR and C4.4A also reflects a certain degree of functional mimicry between these homologous membrane proteins, since rat uPA was reported to interact with rat C4.4A on the cell surface [1]. If this proposition can be taken at face value and be verified in a more rigorous experimental setting it would certainly have wide implications for the concept of cell-surface-associated plasminogen activation catalysed by uPA, since C4.4A could then represent one of the contributory factors responsible for the surprisingly mild overt phenotypes caused by germ-line uPAR deficiency [9,10]. Therefore, we have sought to generate additional evidence to corroborate this proposal using purified

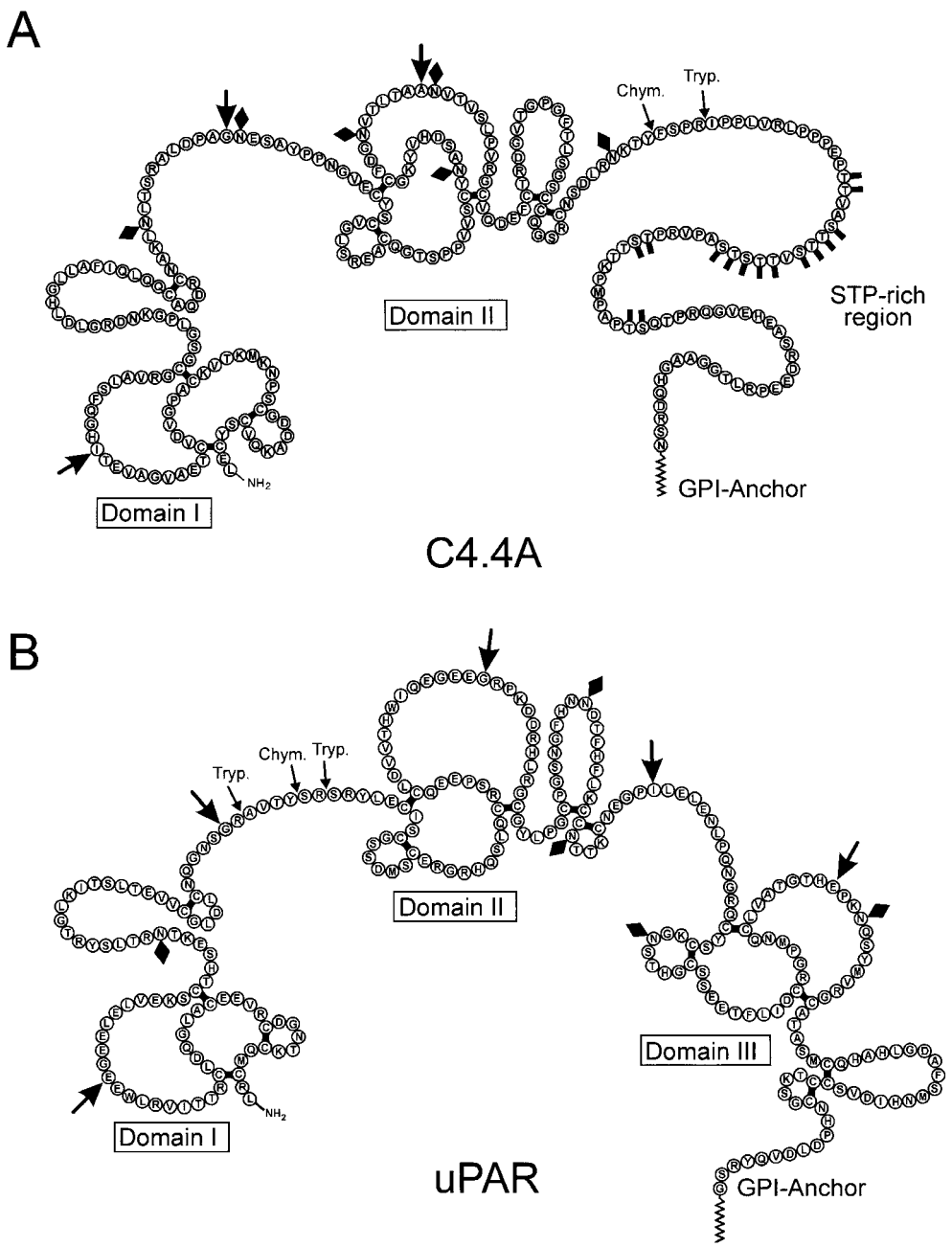

Figure 9 Schematic comparison of the C4.4A and uPAR proteins

Primary structures of C4.4A (**A**) and uPAR (**B**) are shown for comparison using the single letter code. Disulphide bonded cysteines are joint by black bars and their positions were predicted by homology considerations to other members of the Ly6/uPAR/α-neurotoxin protein domain family [5,6]. Diamonds represent potential N-glycosylation sites, pins denote potential O-glycosylation sites (predicted using the NetOGlyc server [26]). The presumed C-terminal attachment site for glycolipid in C4.4A is assigned according to the established rules for such processing [37]. Intron positions in the corresponding genes are highlighted by large arrows (predicted using the NetGene 2 server [38]). Peptide bonds particular sensitive to limited proteolysis with trypsin (Tryp.) or chymotrypsin (Chym.) are identified by small arrows.

components. By surface plasmon resonance analysis we were, however, unable to confirm any interaction between immobilized human C4.4A and either pro-uPA, soluble uPAR or pro-uPA•uPAR complexes at concentrations as high as 200 nM. Likewise, the specific binding of ^{125}I-labelled human uPA to the human breast carcinoma cell line MCF 7, which expresses significant amounts of C4.4A, could be entirely accounted for by a specific engagement of uPAR. If a specific interaction between human uPA and C4.4A were actually to occur despite these observations, it must therefore be of very low affinity and its biological relevance is accordingly questionable. In comparison, the concentration of uPA in normal blood plasma is only 20 pM [34], but the actual concentration of uPA in the interstitial fluids of tissues is difficult to assess due to a local protein synthesis of this protease.

Furthermore, the different expression patterns we observe for C4.4A and uPAR in human term placenta, as well as in the skin during either wound healing or PMA-induced hyperproliferation, are not obviously reconcilable with the proposal of a significant

functional overlap between these homologous proteins. Thus, by immunohistochemistry, we find a substantial expression of C4.4A in the amniotic epithelium of term placenta (see Figure 6), which on the other hand is negative for uPAR [13]. During re-epithelisation of incisional wound in the skin we find a consistent up-regulation of C4.4A in the entire sheet of migrating suprabasal keratinocytes (see Figure 7), which is quite distinct from the focal confinement of uPAR to a few cells in the leading edge of these migrating keratinocytes [16]. Finally, an almost complementary localization of these proteins is observed in the skin 9 h after a single topical application of PMA. This treatment elicits a pronounced up-regulation of C4.4A expression in the suprabasal keratinocytes and in the epithelium of hair follicles, both of which retain undetectable levels of uPAR antigen. An immense infiltration of leucocytes into the dermis upon PMA treatment is the most likely cause for the observed up-regulation of uPAR, but these cells do not express C4.4A. Collectively the biochemical and immunohistochemical data presented do not substantiate the notion of a significant functional overlap between C4.4A and uPAR in these tissues.

In conclusion, it seems highly unlikely that C4.4A can serve as a functional substitute for uPAR in cell-surface-associated plasminogen activation catalysed by uPA. From a functional point of view the GPI-anchored C4.4A is therefore best characterized as an epithelial orphan receptor with an alleged bearing on the progression of human carcinoma [2–4,28]. Recent data from yeast two-hybrid cloning using target libraries isolated from either placenta or a pool of breast cancer-derived cell lines, suggest that human C4.4A may interact with hAG (human anterior gradient)-2 and hAG-3 [28]. These proteins are related to the secreted XAG-2, which is involved in ectodermal differentiation during the early development of *Xenopus laevis* [35]. Additional studies using purified components are required to further substantiate this putative interaction between C4.4A and hAG-2/hAG-3.

We would like to thank Dr M. Zöller (Dept. Tumour Progression and Immune Defence, Heidelberg, Germany) for the gift of the cDNA for human C4.4A, Dr A. L. Jensen (Dept. Protein Chemistry, University of Copenhagen, Denmark) for amino acid composition analysis, Dr N. Behrendt (Finsen Laboratory, Denmark) for lysates of human term placenta, Dr V. Barkholt (Dept. Biochemistry and Nutrition, Technical University of Denmark) for N-terminal protein sequencing, and Dr E. Balslev (Dept. Pathology, Dermatology, and Orthopaedics, Bispebjerg Hospital, Denmark) for sections of chronic human leg ulcers. The excellent technical assistance of Y. deLotto, G. J. Funch, H. Stærmose, P. G. Knudsen, C. L. Jensen and J. Post is gratefully acknowledged. This work was supported by the Danish Cancer Society, Dansk Kræftforskningsfond, Grosserer A. V. Lykfeldt og hustrus Legat, Grosserer Georg Bjørkner og hustru Ellen Bjørkners Fond, Fabrikant Einar Willumsens Mindelegat, Kebmand Johann og Hanne Weimann Legat, EU contract QLG1-CT-2000-01131, and Copenhagen Hospital Corporation (H. S.).

REFERENCES

1 Rosel, M., Claas, C., Seiter, S., Herlevsen, M. and Zoller, M. (1998) Cloning and functional characterization of a new phosphatidyl-inositol-anchored molecule of a metastasizing rat pancreatic tumor. Oncogene **17**, 1989–2002

2 Smith, B. A., Kennedy, W. J., Harnden, P., Selby, P. J., Trejdosiewicz, L. K. and Southgate, J. (2001) Identification of genes involved in human urothelial cell-matrix interactions: implications for the progression pathways of malignant urothelium. Cancer Res. **61**, 1678–1685

3 Wurfel, J., Seiter, S., Stassar, M., Claas, A., Klas, R., Rosel, M., Marhaba, R., Savelyeva, L., Schwab, M., Matzku, S. and Zoller, M. (2001) Cloning of the human homologue of the metastasis-associated rat C4.4A. Gene **262**, 35–41

4 Seiter, S., Stassar, M., Rappl, G., Reinhold, U., Tilgen, W. and Zöller, M. (2001) Upregulation of C4.4A expression during progression of melanoma. J. Invest. Dermatol. **116**, 344–347

5 Ploug, M. and Ellis, V. (1994) Structure–function relationships in the receptor for urokinase-type plasminogen activator. Comparison to other members of the Ly-6 family and snake venom α-neurotoxins. FEBS Lett. **349**, 163–168

6 Ploug, M. (2003) Structure-function relationships in the interaction between the urokinase-type plasminogen activator and its receptor. Curr. Pharm. Des. **9**, 639–652

7 Ploug, M., Rønne, E., Behrendt, N., Jensen, A. L., Blasi, F. and Danø, K. (1991) Cellular receptor for urokinase plasminogen activator. Carboxyl-terminal processing and membrane anchoring by glycosyl-phosphatidylinositol. J. Biol. Chem. **266**, 1926–1933

8 Borglum, A. D., Byskov, A., Ragno, P., Roldan, A. L., Tripputi, P., Cassani, G., Dano, K., Blasi, F., Bolund, L. and Kruse, T. A. (1992) Assignment of the urokinase-type plasminogen activator receptor gene (PLAUR) to chromosome 19q13.1-q13.2. Am. J. Hum. Genet. **50**, 492–497

9 Bugge, T. H., Suh, T. T., Flick, M. J., Daugherty, C. C., Rømer, J., Solberg, H., Ellis, V., Danø, K. and Degen, J. L. (1995) The receptor for urokinase-type plasminogen activator is not essential for mouse development or fertility. J. Biol. Chem. **270**, 16886–16894

10 Dewerchin, M., Nuffelen, A. V., Wallays, G., Bouché, A., Moons, L., Carmeliet, P., Mulligan, R. C. and Collen, D. (1996) Generation and characterization of urokinase receptor-deficient mice. J. Clin. Invest. **97**, 870–878

11 Ploug, M., Kjalke, M., Rønne, E., Weidle, U., Høyer-Hansen, G. and Danø, K. (1993) Localization of the disulfide bonds in the N-terminal domain of the cellular receptor for human urokinase-type plasminogen activator. A domain structure belonging to a novel superfamily of glycolipid-anchored membrane proteins. J. Biol. Chem. **268**, 17539–17546

12 Lund, L. R., Eriksen, J., Ralfkiær, E. and Rømer, J. (1996) Differential expression of urokinase-type plasminogen activator, its receptor, and inhibitors in mouse skin after exposure to a tumor-promoting phorbol ester. J. Invest. Dermatol. **106**, 622–630

13 Pierleoni, C., Samuelsen, G. B., Græm, N., Rønne, E., Nielsen, B. S., Kaufmann, P. and Castellucci, M. (1998) Immunohistochemical identification of the receptor for urokinase plasminogen activator associated with fibrin deposition in normal and ectopic human placenta. Placenta **19**, 501–508

14 Roldan, A. L., Cubellis, M. V., Masucci, M. T., Behrendt, N., Lund, L. R., Danø, K., Appella, E. and Blasi, F. (1990) Cloning and expression of the receptor for human urokinase plasminogen activator, a central molecule in cell surface, plasmin dependent proteolysis. EMBO J. **9**, 467–474

15 Ploug, M., Plesner, T., Rønne, E., Ellis, V., Høyer-Hansen, G., Hansen, N. E. and Danø, K. (1992) The receptor for urokinase-type plasminogen activator is deficient on peripheral blood leukocytes in patients with paroxysmal nocturnal hemoglobinuria. Blood **79**, 1447–1455

16 Solberg, H., Ploug, M., Høyer-Hansen, G., Nielsen, B. S. and Lund, L. R. (2001) The murine receptor for urokinase-type plasminogen activator is primarily expressed in tissues actively undergoing remodeling. J. Histochem. Cytochem. **49**, 237–246

17 Nielsen, B. S., Rank, F., Lopez, J. M., Balbin, M., Vizoso, F., Lund, L. R., Danø, K. and Lopez-Otin, C. (2001) Collagenase-3 expression in breast myofibroblasts as a molecular marker of transition of ductal carcinoma *in situ* lesions to invasive ductal carcinomas. Cancer Res. **61**, 7091–7100

18 Barkholt, V. and Jensen, A. L. (1989) Amino acid analysis: determination of cysteine plus half-cystine in proteins after hydrochloric acid hydrolysis with a disulphide compound as additive. Anal. Biochem. **177**, 318–322

19 Ploug, M., Jensen, A. L. and Barkholt, V. (1989) Determination of amino acid compositions and N-terminal sequences of peptides electroblotted onto PVDF membranes from tricine-sodium dodecyl sulphate-polyacrylamide gel electrophoresis: application to peptide mapping of human complement component C3. Anal. Biochem. **181**, 33–39

20 Gobom, J., Nordhoff, E., Mirgorodskaya, E., Ekman, R. and Roepstorff, P. (1999) Sample purification and preparation technique based on nano-scale reversed-phase columns for the sensitive analysis of complex peptide mixtures by matrix-assisted laser desorption/ionization mass spectrometry. J. Mass Spectrom. **34**, 105–116

21 Ploug, M., Rahbek-Nielsen, H., Nielsen, P. F., Roepstorff, P. and Danø, K. (1998) Glycosylation profile of a recombinant urokinase-type plasminogen activator receptor expressed in Chinese hamster ovary cells. J. Biol. Chem. **273**, 13933–13943

22 Ronne, E., Behrendt, N., Ellis, V., Ploug, M., Dano, K. and Hoyer-Hansen, G. (1991) Cell-induced potentiation of the plasminogen activation system is abolished by a monoclonal antibody that recognizes the N-terminal domain of the urokinase receptor. FEBS Lett. **288**, 233–236

23 Holst-Hansen, C., Johannessen, B., Høyer-Hansen, G., Rømer, J., Ellis, V. and Brunner, N. (1996) Urokinase-type plasminogen activation in three human breast cancer cell lines correlates with their *in vitro* invasiveness. Clin. Exp. Metastasis. **14**, 297–307

24 Petranka, J., Zhao, J., Norris, J., Tweedy, N. B., Ware, R. E., Sims, P. J. and Rosse, W. F. (1996) Structure–function relationships of the complement regulatory protein, CD59. Blood Cells Mol. Dis. **22**, 281–296

25 Grant, G. A., Luetje, C. W., Summers, R. and Xu, X. L. (1998) Differential roles for disulphide bonds in the structural integrity and biological activity of κ-Bungarotoxin, a neuronal nicotinic acetylcholine receptor antagonist. Biochemistry **37**, 12166–12171

26 Hansen, J. E., Lund, O., Nilsson, J., Rapacki, K. and Brunak, S. (1998) O-GLYCBASE Version 3.0: a revised database of O-glycosylated proteins. Nucleic Acids Res. **26**, 387–389
27 Van den Steen, P., Rudd, P. M., Dwek, R. A. and Opdenakker, G. (1998) Concepts and principles of O-linked glycosylation. Crit. Rev. Biochem. Mol. Biol. **33**, 151–208
28 Fletcher, G. C., Patel, S., Tyson, K., Adam, P. J., Schenker, M., Loader, J. A., Daviet, L., Legrain, P., Parekh, R., Harris, A. L. and Terrett, J. A. (2003) hAG-2 and hAG-3, human homologues of genes involved in differentiation, are associated with oestrogen receptor-positive breast tumours and interact with metastasis gene C4.4a and dystroglycan. Br. J. Cancer **88**, 579–585
29 Ploug, M., Ellis, V. and Danø, K. (1994) Ligand interaction between urokinase-type plasminogen activator and its receptor probed with 8-anilino-1-naphthalenesulphonate. Evidence for a hydrophobic binding site exposed only on the intact receptor. Biochemistry **33**, 8991–8997
30 Hoyer-Hansen, G., Behrendt, N., Ploug, M., Dano, K. and Preissner, K. T. (1997) The intact urokinase receptor is required for efficient vitronectin binding: receptor cleavage prevents ligand interaction. FEBS Lett. **420**, 79–85
31 Resnati, M., Pallavicini, I., Wang, J. M., Oppenheim, J., Serhan, C. N., Romano, M. and Blasi, F. (2002) The fibrinolytic receptor for urokinase activates the G protein-coupled chemotactic receptor FPRL1/LXA4R. Proc. Natl. Acad. Sci. U.S.A. **99**, 1359–1364
32 Stephens, R. W., Nielsen, H. J., Christensen, I. J., Thorlacius-Ussing, O., Sørensen, S., Danø, K. and Brunner, N. (1999) Plasma urokinase receptor levels in patients with colorectal cancer: relationship to prognosis. J. Natl. Cancer Inst. **91**, 869–874
33 Mustjoki, S., Sidenius, N., Sier, C. F., Blasi, F., Elonen, E., Alitalo, R. and Vaheri, A. (2000) Soluble urokinase receptor levels correlate with number of circulating tumor cells in acute myeloid leukemia and decrease rapidly during chemotherapy. Cancer Res. **60**, 7126–7132
34 Grondahl-Hansen, J., Agerlin, N., Munkholm-Larsen, P., Bach, F., Nielsen, L. S., Dombernowsky, P. and Dano, K. (1988) Sensitive and specific enzyme-linked immunosorbent assay for urokinase-type plasminogen activator and its application to plasma from patients with breast cancer. J. Lab. Clin. Med. **111**, 42–51
35 Aberger, F., Weidinger, G., Grunz, H. and Richter, K. (1998) Anterior specification of embryonic ectoderm: the role of the *Xenopus* cement gland-specific gene *XAG-2*. Mech. Dev. **72**, 115–130
36 Altmann, F., Staudacher, E., Wilson, I. B. and Marz, L. (1999) Insect cells as hosts for the expression of recombinant glycoproteins. Glycoconj. J. **16**, 109–123
37 Udenfriend, S. and Kodukula, K. (1995) How glycosylphosphatidylinositol-anchored membrane proteins are made. Annu. Rev. Biochem. **64**, 563–591
38 Brunak, S., Engelbrecht, J. and Knudsen, S. (1991) Prediction of human mRNA donor and acceptor sites from the DNA sequence. J. Mol. Biol. **220**, 49–65

Received 26 September 2003/24 February 2004; accepted 10 March 2004
Published as BJ Immediate Publication 10 March 2004, DOI 10.1042/BJ20031478